Sucrose or starch? The influence of tonoplast sucrose transporter perturbation on carbon partitioning for growth, defense, and winter protection in coppiced poplar

Trevor T. Tuma[1], Batbayar Nyamdari[1], Chen Hsieh[2], Yen-Ho Chen[3], Scott A. Harding[1,4], & Chung-Jui Tsai[1,2,3,4]

[1] Warnell School of Forestry and Natural Resources, University of Georgia, Athens, GA, 30602, USA.

[2] Institute of Bioinformatics, University of Georgia, Athens, GA, 30602, USA.

[3] Department of Plant Biology, University of Georgia, Athens, GA, 30602, USA.

[4] Department of Genetics, University of Georgia, Athens, GA, 30602, USA.

Key words: sucrose transporter, Populus, CRISPR, carbohydrates, metabolism, coppicing, remobilization

Running head: SUT4 and seasonal carbohydrate reserve partitioning

Corresponding author: Chung-Jui Tsai (cjtsai@uga.edu)

Abstract

Non-structural carbohydrate reserves of stems and roots underpin overall tree fitness as well as productivity under short-rotation management practices such as coppicing for bioenergy. While both sucrose and starch comprise the predominant carbohydrate reserves of *Populus*, utilization is understood primarily in terms of starch turnover. The tonoplast sucrose transport protein SUT4 modulates sucrose export to distant sinks, but the possibility of its involvement in sink tissue carbohydrate remobilization has not been explored. Here, we used *PtaSUT4*-knockout mutants of *Populus tremula* × *alba* (INRA 717-1B4) in winter and summer glasshouse coppicing experiments to strain carbon demand and test for SUT4 involvement in reserve utilization. We show that epicormic bud emergence was delayed and subsequent growth reduced in *sut4* mutants following winter but not summer coppicing. Reserve depletion during post-coppice regrowth was not impaired in the *sut4* mutants under winter or summer glasshouse conditions. Interestingly, xylem hexose increased during post-coppice growth exclusively in the winter when osmoprotection is critical, and the increase was attenuated in *sut4* mutants. Accrual of abundant defense metabolites, including salicinoids, chlorogenic acids, and flavonoid products was prioritized in the summer, but conspicuously lower in *sut4* mutants than controls. Together, our results point to shifting priorities for SUT4 function from support for osmoprotection in winter to chemical defense in summer. Delayed bud release and growth following winter but not summer coppicing in the *sut4* mutants demonstrate the importance of SUT4 in modulating trade-offs between growth and the other priorities during reserve utilization in *Populus*.

Introduction

Renewable energy production from feedstock like tree crops is expected to help reduce fossil fuel use and greenhouse gas emissions responsible for global warming (Ragauskas *et al.*, 2006, Dhillon & von Wuehlisch, 2013, Nieminen *et al.*, 2012). *Populus* species (e.g., poplar, aspen, cottonwood, and their respective hybrids) have proven useful for this purpose due to their fast growth, high biomass production, and ability to grow in marginal environments (Bryant *et al.*, 2020, Kauter *et al.*, 2003, Chudy *et al.*, 2019). Coppicing, where trees are harvested near ground level and new shoots regenerate from the stool for repeated harvesting without replanting, is a common practice in short-rotation woody biomass production (Tschaplinski & Blake, 1989). Feedstock biomass yields from coppicing can rival those of trees grown from seedlings or cuttings (Labrecque *et al.*, 2023, Proe *et al.*, 1999).

The success of coppicing is influenced by the composition and utilization of non-structural carbohydrate reserves available from sink organs for new growth (Luostarinen & Kauppi, 2005, Karp & Shield, 2008). The carbohydrate reserves facilitate not only bud emergence and new shoot growth in the spring before source organ photosynthesis becomes active, but also after defoliation or stem girdling events (Regier *et al.*, 2010, Falk *et al.*, 2020, Gleason & Ares, 2004). In general, it is considered that both soluble sugars and starch comprise storage reserves, with exchange between the constituent pools occurring on daily and seasonal time-scales in trees (Tixier *et al.*, 2018, Martínez-Vilalta *et al.*, 2016). It is widely held that reserve dynamics are important to trade-offs between storage, growth, defense, and protection, all of which influence tree fitness (Blumstein *et al.*, 2022). Genetics and plasticity both contribute to these trade-offs

70 (Herms & Mattson, 1992). Genetic variation in carbohydrate storage and utilization has been
71 explored to greater depth for annual food crops since digestibility, storability, and flavor can
72 depend on reserve carbohydrate transformations (Baxter *et al.*, 2005, Sekhon *et al.*, 2016, Li *et*
73 *al.*, 2005). In the case of trees, however, the molecular mechanisms by which non-structural
74 carbohydrate reserves contribute to new vegetative growth are relatively under-described.
75
76 Starch is regulated diurnally (Hartmann & Trumbore, 2016, Noronha *et al.*, 2018, Klein & Hoch,
77 2015), and therefore has been the focus of most studies on reserve carbohydrate utilization.
78 However, significant diurnal fluctuations in leaf sucrose reserves occur in *Populus* (Wang *et al.*,
79 2022, Zhang *et al.*, 2014). Recent evidence suggests that in the absence of starch, other
80 carbohydrates, presumably including sucrose, can provide the reserves needed to sustain new
81 vegetative growth (Wang et al., 2022). Under extreme carbon limitation, carbohydrate storage
82 can supersede growth as a priority (Wang et al., 2022, Wiley *et al.*, 2019, Sala *et al.*, 2012, Piper
83 & Fajardo, 2016, Huang *et al.*, 2021). Under such conditions, trees may rely instead on
84 alternative substrates such as lipids (Huang et al., 2021, Fischer *et al.*, 2015) and hemicelluloses
85 (Schädel *et al.*, 2009) to sustain respiration and growth. It is worth noting that phenolic glycoside
86 salicinoids, which are abundant defense compounds in *Populus* species, are turnover-resistant
87 during severe carbon deprivation (Hillabrand *et al.*, 2023). This highlights the importance of
88 chemical defense in relation to growth and storage as a carbon destination in these species. Given
89 the diverse metabolic and osmotic demands that potentially govern competition for sucrose,
90 limited attention has been given to the physiological importance of its dynamic
91 compartmentalization.
92

93 Transmembrane sucrose transporters (SUTs) facilitate the movement of sucrose in all plants
94 (Kühn *et al.*, 1999, Ayre, 2011). Several phylogenetically and subcellularly distinct isoforms are
95 known (Peng *et al.*, 2014), but in *Populus*, *SUT4* encoding the tonoplast isoform is expressed at a
96 relatively high level compared to most other *SUTs* throughout the plant (Payyavula *et al.*, 2011).
97 SUT4 facilitates sucrose export from the vacuole to the cytosol, and its manipulation affects
98 tissue sucrose abundance (Payyavula et al., 2011, Eom *et al.*, 2011, Schneider *et al.*, 2012). In
99 addition, *SUT4* is expressed in overwintering sink organs of several temperate tree species
100 including *Populus* (Dobbelstein *et al.*, 2018, Ko *et al.*, 2011), and its expression varies in
101 accordance with abiotic stress (Xu *et al.*, 2017, Payyavula et al., 2011, Frost *et al.*, 2012, Harding
102 *et al.*, 2022). Effects of *SUT4* silencing or knockout (KO) on source leaf turgor control and starch
103 homeostasis have also been reported (Harding *et al.*, 2020, Harding et al., 2022).
104
105 These observations are all consistent with the general notion that SUT4 may be involved with the
106 control of carbohydrate utilization in sink organs of *Populus*. Here, we used coppicing as a tool
107 to investigate whether tonoplast sucrose trafficking is important for sink organ function under
108 carbon-limiting conditions. A *SUT4*-KO effect on resprouting or defense metabolite investments
109 would imply that physiological trade-offs are governed by the export of vacuolar sucrose *per se*,
110 rather than export as its component hexoses or other modified forms. We compared epicormic
111 bud growth in the contexts of stool metabolism, chemical defense, and osmolyte maintenance to
112 test for SUT4 importance to both summer and winter tradeoffs between growth, storage, defense,
113 and winter protection.
114
115

116 **Materials and Methods**

117

118 **Plant production and maintenance**

119 *PtaSUT4*-KO mutants and the *Cas9* empty vector control lines used in this study were generated
120 by CRISPR/Cas9 mutagenesis as reported previously (Zhou *et al.*, 2015, Harding et al., 2022)
121 and grown in a glasshouse located in the Whitehall Forest at the University of Georgia.
122 Supplemental LED lighting was used to maintain a 16-hour photoperiod, with photosynthetic
123 photon flux density of at least 600 µmol m^{-2} s^{-1} at mid canopy. Plants were propagated by single-
124 node cuttings as described (Frost et al., 2012) year-round for the experiments. Once established,
125 rooted propagules were transferred to 1-gallon pots containing commercial soil mix (Fafard 3B)
126 supplemented with Osmocote (15-9-12, NPK 6-month slow release) and maintained with daily
127 watering until coppicing.

128

129 **Coppicing experiments**

130 For the winter coppicing experiment (January), twelve control (six wild-type [WT] and six *Cas9)*
131 and twelve *sut4* mutants (four plants each of three independent events: KO-18, KO-25, and KO-
132 51), were equally and randomly spaced on the floor bench of the glasshouse. Ten days prior to
133 coppicing, the number of fully expanded leaves was reduced to forty for each plant to minimize
134 differences in water uptake and photosynthetic capacity. Plants ~1.5 m in height were then
135 coppiced (Julian Day 18) to ~25 cm stumps and any remaining leaves were removed. Watering
136 was reduced after coppicing to avoid root anoxia. Outdoor temperatures during the duration of
137 the winter coppicing experiment ranged from -5°C to 16°C, with an average of 6.5°C. Day

138 length ranged from 10.2 hours to 10.7 hours. Supplemental heating prevented indoor glasshouse
139 temperatures from dropping below 10°C.
140
141 For the summer coppicing experiment (August), plants were managed as described above and
142 were approximately the same height at coppicing as those in the winter experiment. Ten control
143 plants (six WT and four *Cas9)* and twelve *sut4* mutants (four plants each of KO-18, KO-25, and
144 KO-51 as above), were coppiced (Julian Day 228). Outdoor temperatures during the duration of
145 the summer coppicing experiment ranged from 20°C to 33°C, with an average of 26°C. Day
146 length ranged from 12.9 to 13.4 hours. Evaporative cooling prevented glasshouse temperatures
147 from exceeding a high of 35°C during the day. The coppicing experiments were carried out twice
148 to ensure reproducibility. Results from the most comprehensive of the two experiments are
149 reported here.
150
151 **Pre- and post-coppice sampling**
152 Immediately before coppicing, deveined lamina of two adjacent fully-expanded source leaves,
153 *i.e.*, Leaf Plastochron Index (LPI) 15-16, were flash frozen in liquid N and stored at -80ºC for
154 analyses. Immediately after coppicing (t=0), xylem sap was collected from the cut surfaces of the
155 stools. Bark and xylem tissues were collected from the top of the stump immediately after sap
156 collection (t=0; Supplemental Figure S1) and again when epicormic bud elongation was
157 measured (t=1; Supplemental Figure S1). The third and final sampling (t=2) took place during
158 shoot extension. Tissues were snap frozen in liquid N and stored at -80°C. At t=2, root samples
159 (terminal 6 cm of elongating roots excluding root tips) were washed in deionized water, dried,
160 and snap frozen in liquid N. The largest (dominant) epicormic bud that emerged after coppicing

161 of each tree was photographed and its length determined at t=1 using the ImageJ software
162 package (https://imagej.net/ij/index.html). Due to seasonal growth differences, sampling at times
163 t=1 and t=2 was carried out 10 and 16 days, respectively, after summer coppicing and 11 and 20
164 days, respectively, after winter coppicing (Supplemental Figure S1). All tissue sampling
165 occurred under sunny conditions between 11AM – 2PM.
166
167 **Biomass**
168 A second coppicing experiment was carried out to determine biomass of shoots produced from
169 stumps ~1 month after coppicing. For this, coppicing of ~1.0 m plants (n = 6 – 12) was carried
170 out in winter (December) and summer (June). Leaves (including petioles) and shoot tissues were
171 dried in a forced air oven for 48 hours at 60°C. Independently of the coppicing experiments,
172 cohorts of mature (~2 m) control and *sut4* mutant plants (n = 8 – 14 plants) were harvested in
173 mid-winter (January) and mid-summer (July-August) for whole plant dry biomass analysis. Plant
174 height and stem diameter were measured at harvest, and leaves (including petiole), bark, and
175 wood (de-barked stem) were collected to determine biomass allocation patterns. Root tissues
176 were washed in deionized water and dried.
177
178 **Xylem sap**
179 Xylem sap was collected from the stumps immediately after coppicing following a previously
180 published approach (Siebrecht & Tischner, 1999). Bark was removed from the top 4 cm of the
181 stump to expose the xylem cylinder and to avoid mixing of phloem and xylem sap during
182 collection. The razor-cut surface of the wood was tamped clean with a damp kimwipe. The first
183 400 µl of xylem sap was discarded. Over the next 45 min, ~100-200 µl of xylem sap was

184 collected with a pipette from each stump and snap frozen in liquid nitrogen. Frozen sap was
185 stored at -80°C, thawed on ice just before analysis, mixed, and derivatized after drying in glass
186 inserts for metabolite analysis as described below.
187
188 **Metabolite analysis**
189 Tissues were freeze-dried using a FreezeZone 2.5 (Labconco), Wiley milled through a 40-mesh
190 sieve (Thomas Scientific), and further ball-milled at 1500 rpm in a MiniG tissue homogenizer
191 (Spex SamplePrep) to a fine powder. An aliquot of tissue powder (10.0 ± 0.5 mg) was used for
192 metabolite profiling by gas chromatography-mass spectrometry (GC-MS) as detailed in Harding
193 et al. (2022). Adonitol (Sigma-Aldrich) was used as an internal standard. Samples were analyzed
194 on an Agilent 7890A GC coupled to an Agilent 5975C single quadrupole MS detector (Agilent
195 Technologies). Peaks were deconvoluted using AnalyzerPro (SpectralWorks) and putative
196 identities were assigned based on the NIST08, the Agilent Fiehn metabolomics library, and an
197 in-house library of authentic standards (Harding et al., 2022). A standard mix containing succinic
198 acid, sucrose, glutamic acid, fructose, glucose, and ascorbic acid was loaded at the beginning and
199 end of each sample set to monitor derivatization and instrument performance.
200
201 Another tissue powder aliquot (5.0 ± 0.5 mg) was used for profiling by ultra-performance liquid
202 chromatography coupled with quadrupole time-of-flight mass spectrometry (UPLC-QTOF).
203 Tissue extraction was performed as above (Harding et al., 2022) with the exception that $^{13}C_6$ –
204 cinnamic acid and D_5–benzoic acid were included as internal standards. Extracts were filtered
205 through a 0.2 μm PTFE (polytetrafluoroethylene) filter (Agilent Technologies) and resolved on
206 an Agilent Zorbax Eclipse Plus C18 column (2.1 × 50 mm, 1.8 μm) using an Agilent 1290

207 Infinity II UPLC coupled to an Agilent 6546 LC/Q-TOF tandem MS. The mobile solvent A
208 comprised water and 0.1% formic acid and mobile solvent B comprised acetonitrile with 0.1%
209 formic acid at a flow rate of 0.5 mL min^{-1}. The elution gradient was 3% B from 0 – 0.5 min,
210 linear gradient to 15% B over 3.5 min, isocratic at 30% B over 4.5 min, linear gradient to 50% B
211 over 5.5 min, and then to 100% B over 7 min, followed by a 3-min post-column run. Column
212 temperature was 45°C. MS data were acquired in negative mode with the following parameters:
213 gas temperature, 250°C; nebulizer gas, 40 psi; nozzle voltage, 500 V; and capillary voltage, 400
214 V. Data were processed using the MassHunter software suite Version 11.0 (Agilent). Peak
215 identities were confirmed using an in-house library of authentic standards, when available, or
216 assigned by searching against an accurate-mass NIST20 library. The highest database match
217 score (usually >85%) obtained was used to support the putative identity of the QTOF
218 metabolites.
219
220 GC-MS and LC-QTOF peak intensities were normalized by their respective internal standards
221 and sample dry weight, with the exception of tissue sucrose and hexose (fructose and glucose)
222 levels which are reported as percent dry weight based on their respective calibration curves.
223
224 **Starch**
225 Starch content was determined by enzymatic digestion with α-amylase and amyloglucosidase
226 (Chow & Landhäusser, 2004). In brief, 10 mg of lyophilized, Wiley- and ball-milled tissue
227 powder was pre-extracted three times with 1 ml of methanol by vortexing and sonication. The
228 tissue pellet was resuspended in 0.5 ml of buffer (0.1 M sodium acetate, pH 5.0, with 5 mM
229 $CaCl_2$) containing 500 U of α-amylase (Sigma A4551) and incubated for 2 hr at 65°C. Samples

230 were cooled and 10 µl of sodium acetate buffer (pH 5.0) containing 5 U amyloglucosidase
231 (Sigma A1602) was added for further digestion at 50°C for 48 hr with shaking. Digests were then
232 diluted with 500 µl of H_2O, vortexed, centrifuged, and 20 µl of the diluted supernatant were
233 dried and derivatized for GC-MS as described above. Chromatograms contained only glucose
234 and adonitol internal standard peaks. Total starch content was calculated based on a glucose
235 standard curve and expressed as µg starch per mg of dry tissue.
236
237 **Condensed tannins (CTs)**
238 Freeze dried tissue powder (10 mg) was extracted in 600 µl of methanol for 15 minutes in a
239 sonicator bath to extract interfering chlorophyll. The depigmented pellet was dried and CT
240 content was estimated using the butanol-HCl method (Porter *et al.*, 1986) as described (Harding
241 et al., 2022). CT concentration was determined based on absorbance at 550 nm (SpectraMax M2;
242 Molecular Devices) using purified aspen leaf CTs as standards.
243
244 **Chlorophyll content**
245 Ten mg of freeze-dried powder was extracted twice in 750 µl of cold 90% acetone – 10% water,
246 with sonication and centrifugation. Absorbances at 645 nm and 663 nm were used to determine
247 chlorophyll *a*, chlorophyll *b*, and total chlorophyll content (µg g^{-1} DW) as described by
248 Lichtenthaler (1987).
249
250 **Statistics**
251 Repeated measures analysis of variance (ANOVA) was used to determine significant differences
252 at each stage of coppicing re-growth over time, between genotypes, and their interactions using *R*

253 v4.1.0 in Rstudio (version 2022.12.353). Linear regression was used to test for the relationships
254 between sucrose or starch depletion and bud elongation of WT or *sut4* mutants between t=0 and
255 t=1 of the winter and summer coppicing experiments.
256
257
258 **Results**
259
260 *Seasonal coppicing response of sut4 mutants*
261 We conducted coppicing experiments to study sink organ carbohydrate utilization under both
262 short-day, cool winter conditions and long-day, warm summer conditions in a glasshouse (Figure
263 S1). The rate at which new epicormic buds appeared on stumps after coppicing was largely
264 similar between genotypes under the summer glasshouse conditions (Figure 1A, C). The total
265 biomass of new shoots at t=2 in the *sut4* mutants was also similar to the controls despite initially
266 faster bud elongation in *sut4* mutants (t=1) during the summer (Figure 1E-F). By contrast,
267 epicormic bud release was delayed by several days in *sut4* mutants compared to controls in the
268 winter but attained the same number of sprouts by t=2 (Figure 1B, D). Bud elongation at t=1 was
269 slower and total biomass at t=2 was reduced in the *sut4* mutants compared to control plants
270 following winter coppicing (Figure 1E-F). A replicate experiment was conducted to examine
271 biomass partitioning in fully-grown new shoots 32 and 40 days after summer and winter
272 coppicing, respectively. Total leaf and stem dry mass were significantly higher in *sut4* than
273 control sprouts under summer conditions (Table 1). In contrast, total biomass trended lower, but
274 not significantly, in *sut4* than in control plants in the winter (Table 1), which translates to overall
275 less robust coppice growth of *sut4* mutants in the winter than summer. The seasonal differences

276 in biomass allocation of coppices were not observed in mature trees (t=0) which showed slight
277 shoot biomass reductions in both seasons (Table S1), similar to previously reported for *SUT4*-
278 silenced trees (Frost et al., 2012, Harding et al., 2020, Payyavula et al., 2011). The results hint at
279 a seasonal influence of SUT4 on coppicing responses.
280
281 *Sink carbohydrate reserves*
282 Sucrose contents of mature tree organs were higher in the *sut4* mutants when compared to the
283 controls (Figure S2), as reported previously (Harding et al., 2022). Following summer or winter
284 coppicing, bark and xylem sucrose abundance generally decreased (Figure 2A). The decrease
285 was less marked in *sut4* than control by t=2 of the summer experiment, but sucrose was depleted
286 to approximately the same low abundance in bark and xylem of both genotypes under winter
287 conditions (Figure 2A). Root sucrose was not as depleted by coppicing and remained higher in
288 *sut4* than control lines at t=2, especially in the summer (Figure 2A).
289
290 Bark hexose (sum of fructose and glucose) levels differed little between genotypes and decreased
291 by t=2 in both the summer and the winter (Figure 2B). In contrast, xylem hexose levels increased
292 in both lines in the winter between t=0 and t=2, but decreased in the summer by t=2 (Figure 2B).
293 In both seasons, but most notably in the winter, xylem hexose levels were higher in control than
294 *sut4* mutants. Root hexose levels increased sharply in both genotypes after summer coppicing,
295 but the increase was observed only in control plants after winter coppicing (Figure 2B).
296
297 Starch levels in the bark and xylem were higher in control than *sut4* plants in both the summer
298 and winter, and remained so as starch decreased through t=1 (Figure 2C). Bark and xylem starch

299 was depleted to similarly low levels in both genotypes by t=2, suggesting that starch abundance
300 there had reached a minimum. Root starch content was similar in both genotypes at t=2 but was
301 much less abundant in the summer than the winter (Figure 2C). Together, the data suggest a
302 depletion of non-structural carbohydrates to less than 25% of pre-coppice levels, in shoot organs.
303 Root sucrose also decreased sharply, but starch was only measured at final harvest (t=2).
304
305 *Sucrose and starch utilization for bud growth*
306 Slower post-coppice sprout emergence and growth in *sut4* than control trees in the winter led us
307 to test whether sucrose and/or starch depletion between t=0 and t=1 in the bark predicted bud
308 length at t=1 (Figure 3). Bud size did not correlate with sucrose depletion in the summer for
309 either genotype (*sut4:* r^2 = 0.17, p = 0.21, control*:* r^2 = 0.06, p = 0.49), but the slope trended
310 positive for *sut4* and negative for control plants (Figure 3A). Under winter conditions, bud length
311 correlated with sucrose depletion in the *sut4* mutant trees (r^2 = 0.39, p = 0.03) but not in the
312 controls (r^2 = 0.16, p = 0.19) where in fact the slope trended negative as in winter (Figure 3A).
313 Bud expansion did not correlate with changes in starch content under summer (*sut4:* r^2 = 0.02, p
314 = 0.68, control*:* r^2 = 0.12, p = 0.439) or winter (*sut4:* r^2 = 0.00, p = 0.99, control*:* r^2 = 0.04, p =
315 0.54) conditions (Figure 3B). Overall, post-coppice bud elongation in *sut4* mutant, but not in
316 control plants, tended to correlate positively with sucrose but not with starch depletion. While
317 bud growth was slower in *sut4* than control plants in the winter, sucrose depletion in *sut4* reserve
318 organs was normal. Other factors related to sucrose utilization may have led to the appearance
319 suggested in the regressions (Figure 3) of a sucrose limitation to *sut4* bud growth.
320
321 *Xylem sap and root metabolites*

322 Xylem sap sucrose abundance at t=0 was greater in winter than summer, but differed little
323 between genotypes during either season (Figure 4A). Sap hexose levels did not differ between
324 genotypes in the summer but were reduced in *sut4* compared to control plants in the winter
325 (Figure 4B). Xylem sap is also the route by which most root-assimilated nitrogen travels to the
326 transpiring leaves (Siebrecht & Tischner, 1999). Given that nitrogen assimilation depends on
327 carbon skeletons in the assimilating organ, a comparison of xylem sap Krebs cycle intermediate
328 and amino acid contents could reveal seasonal and genotypic differences in systemically
329 available carbon in the roots. Krebs cycle intermediates malate and citrate comprised most of the
330 xylem sap metabolic load in both summer and winter, and were more abundant in *sut4* than
331 control xylem saps (Figure 4C-D). Glutamine and glutamate were the most abundant amino acids
332 we detected in xylem sap. Both trended higher in *sut4* than control xylem sap in the summer but
333 were significantly lower in *sut4* than control sap in the winter (Figure 4C-D). These four
334 metabolites were also among the most abundant in root tissues, but only malate mimicked the
335 xylem sap patterns, being most abundant in *sut4* (Supplemental Figure S3).
336
337 *Bark and xylem primary metabolites*
338 Bark and xylem metabolite response trends at t=0 roughly paralleled those observed in xylem
339 saps, with amino acids being lower and Krebs cycle intermediates higher in *sut4* mutants, most
340 markedly in winter xylem (Figure 5). Malate and citrate were more abundant in *sut4* than control
341 bark and xylem during the winter, with the differential increasing during bud expansion (t=1 and
342 t=2) (Figure 5). Phenylpropanoid pathway precursors (e.g., quinic acid and shikimic acid) and
343 intermediates (e.g., hydroxycinnamates and catechin) were detected at comparatively low levels
344 in *sut4* bark and xylem throughout the course of both seasons. Finally, levels of stress

345 metabolites and sugar alcohols including raffinose, galactinol and myo-inositol were generally
346 greater in the bark of mature *sut4* plants (t=0) but lower than in controls by t=2 (Figure 5).
347
348 *Chemical defense*
349 Provisioning of nonstructural sinks related to poplar defense has been associated with
350 carbohydrate transport (Arnold *et al.*, 2004, Kleiner *et al.*, 1999). In *Populus* and *Salix* species,
351 chlorogenic acids, salicinoids (e.g., salicortin and tremulacin), and CTs derived from quinate-
352 shikimate-phenylpropanoid pathway are present in especially large abundance for fitness and
353 stress tolerance (Harding *et al.*, 2005, Tsai *et al.*, 2006, Zhang *et al.*, 2018). Chlorogenic acids
354 (caffeoyl-quinate isomers) were at lower levels in *sut4* relative to control bark at all time points
355 in both the summer and winter coppicing experiments (Figure 6A). Salicortin, by far the most
356 abundant defense metabolite, was detected at higher levels in the summer than the winter (Figure
357 6B). Bark salicortin abundance was substantially lower in the *sut4* mutants than control during
358 the summer but did not differ between genotypes during the winter (Figure 6B). The closely
359 related tremulacin was also significantly lower in *sut4* mutant bark in the summer, but not the
360 winter (Figure 6C). Bark CT levels were lower in *sut4* than control plants, especially in the
361 summer (Figure 6D).
362
363 *Chlorophyll content*
364 We examined bark chlorophyll contents as proxies for photosynthetic capacity after coppicing.
365 Bark chlorophyll content differed little between genotypes and remained relatively stable during
366 summer coppicing experiment, but showed a transient decrease at t=1 during winter (Figure 7).
367

368 **Discussion**

369

370 Trees produce nonstructural carbohydrate reserves to sustain respiration and osmoregulation for
371 winter protection and spring bud flush during perennial growth (Furze *et al.*, 2019). The
372 plasticity of reserve utilization across species is well documented and probably reflects multiple
373 environmental and genetic influences over the process (Sevanto *et al.*, 2014, Blumstein et al.,
374 2022, Martínez-Vilalta et al., 2016, Furze et al., 2019). While it is generally assumed that starch
375 comprises the bulk of metabolically available reserve carbohydrate, this is mainly inferred from
376 the diurnal accrual and depletion of transient starch in annual species (Smith & Stitt, 2007).
377 However, a process as fundamental as bud flush in aspen can occur in the absence of starch
378 (Wang et al., 2022). Therefore, reserve carbohydrate accrual and utilization exhibits plasticity
379 and can proceed through multiple routes. An analysis of carbohydrate active gene expression in
380 overwintering stem tissue of poplar supports involvement of starch degradation as well as of
381 sucrose synthesis and trafficking (Figure S4) (Ko et al., 2011). Several studies report sustained
382 winter expression of sucrose transporters in tree sink organs, with gene transcript levels for the
383 tonoplast sucrose transporter *SUT4* peaking in the winter (Figure S4) (Dobbelstein et al., 2018,
384 Ko et al., 2011). Therefore, it is likely that sucrose trafficking and starch metabolism are
385 important for winter survival.

386

387 Under winter post-coppice conditions in the present study, stump starch and sucrose were
388 reduced to 14% and 17% of their initial levels in control and mutant lines, respectively, but
389 epicormic bud growth was slow in *sut4* mutants compared to controls. It is probable that sucrose
390 trafficking increases in importance during the winter in line with reports of higher *SUT4* gene

391 expression in winter (Figure S4) (Dobbelstein et al., 2018, Ko et al., 2011). Stump sucrose levels
392 were higher in winter than summer as others have reported (Furze et al., 2019), but reduced *sut4*
393 bud elongation only in winter could suggest growth-hindering injury or stress of some sort.
394
395 It is worth considering that cytosolic sucrose sustains critical winter processes such as hexose
396 production for non-nutritive purposes. We observed that xylem hexose levels increased in
397 coppiced stumps in the winter, but not in the summer in all lines, and that the levels were overall
398 lower in *sut4* mutants (Figure 2B). Hexose osmolytes in the xylem could represent a high priority
399 allocation of nonstructural carbohydrates for winter protection. This is consistent with the
400 previously established roles of sugar osmolytes in reactive oxygen species scavenging, cold
401 tolerance, and embolism refilling during winter (Charrier *et al.*, 2018, Tarkowski & Van den
402 Ende, 2015), and with abundant expression of cell wall invertases in winter stems (Ko et al.,
403 2011). Our finding that both xylem hexose and bud growth were compromised in *sut4* raises the
404 possibility that reduced cytosolic sucrose metabolism may have been injurious to the winter
405 stumps. Besides the overall reduction in hexose, reductions in other important sucrose-derived
406 protective osmolytes like raffinose were also observed in *sut4* compared to control stumps
407 (Figure 5). A similar effect on raffinose was reported in leaves of drought-stressed poplar lines
408 with reduced *SUT4* gene expression (Frost et al., 2012). The data suggest active participation of
409 SUT4 during utilization of winter carbohydrate reserves for both growth and injury avoidance.
410
411 As in xylem, root hexose was detected at lower levels in *sut4* than control coppices in the winter
412 at t=2. In root and xylem cells alike, sucrose that is exported from the vacuole is converted to
413 hexoses by cytosolic and apoplastic cell wall invertases (Koch, 2004, Ruan, 2014). Utilization of

414 sucrose that is not exported from the vacuole depends on the activity of vacuolar invertase and
415 tonoplast hexose transporters (Koch, 2004, Ruan, 2014, Schulz *et al.*, 2011). Their expression is
416 modulated by stresses, such as drought and cold (Wormit *et al.*, 2006, Roitsch & González, 2004,
417 Chen *et al.*, 2015, Xue *et al.*, 2016). Post-coppicing invertase gene expression likely varied due
418 to seasonal differences in soil moisture and temperatures, resulting in more harmful
419 consequences of *sut4* limitation in winter than in summer. The finding that root hexose increased
420 sharply and equally in both control and mutant lines after summer coppicing, but did not increase
421 in *sut4* after winter coppicing supports this interpretation.
422
423 In summer, the metabolic priority of coppices seemed to shift toward increased accrual of
424 resource-intensive poplar defense metabolites such as chlorogenic acids, salicortin, and CTs.
425 This is consistent with a greater depletion of sucrose and starch in control (to 6% of initial levels)
426 than in *sut4* (to below 23%) in the summer. While epicormic bud emergence was similar in all
427 lines following summer coppicing, defense metabolite levels were substantially lower and new
428 sprout biomass was significantly higher in *sut4* than control lines. *Populus* species maintain
429 constitutive levels of salicinoids even under severe carbon limitation (Hillabrand et al., 2023,
430 Fabisch *et al.*, 2019), but our results suggest that growth can be prioritized over defense under
431 sufficiently carbon limiting conditions, at least when trafficking of vacuolar sucrose is impaired.
432
433 In conclusion, PtaSUT4 was revealed through seasonal differences in the coppicing responses of
434 KO mutant lines to have a role in nonstructural carbohydrate allocations for growth and winter
435 protection. Future research may investigate the effects of *SUT4*-KO under field conditions to
436 further explore seasonal influences on SUT4 function and perennial growth habit.

Data and Materials Availability: Data and material will be made available upon reasonable request.

Supplemental data

Table S1. Biomass allocation of mature control and *sut4* poplar.

Figure S1. Schematics of coppicing experiments.

Figure S2. Sucrose levels in mature tree organs.

Figure S3. Root metabolites.

Figure S4. Seasonal variation of *SUT* and representative carbohydrate gene expression.

Conflict of interest: None declared.

Funding: This work was supported in part by a National Science Foundation Graduate Research Fellowship (DGE – 1842396) to T.T.T., a Department of Energy, Office of Science, Biological and Environmental Research Program Award (DESC0023166) to C.J.T., and the Georgia Research Alliance Hank Haynes Forest Biotechnology endowment to C.J.T. Funding for the Agilent UPLC-QTOF was provided by the U.S. Department of Agriculture, National Institute of Food and Agriculture, Equipment Grant Program (Award 2021-70410-35297 to C.J.T. and S.A.H.).

Acknowledgements: The authors thank Gilles Pilate of INRA, France for providing poplar clone INRA 717-1B4, Suzzanne Tate for greenhouse assistance, and Khadijeh Mozaffari for LC-QTOF assistance.

Authors' Contributions: T.T.T, S.A.H, & C-J.T. conceived the study and designed all experiments. T.T.T. performed all experiments and analyzed the data. T.T.T, B.N., & S.A.H, performed metabolic analyses. Y-H.C. and C.H. helped with expression analysis. T.T.T. prepared the draft manuscript, which was edited by S.A.H. and C-J. T.

References

Arnold, T., Appel, H., Patel, V., Stocum, E., Kavalier, A. and Schultz, J. (2004) Carbohydrate translocation determines the phenolic content of Populus foliage: a test of the sink-source model of plant defense. *New Phytologist,* **164,** 157-164.

Ayre, B. G. (2011) Membrane-transport systems for sucrose in relation to whole-plant carbon partitioning. *Molecular Plant,* **4,** 377-394.

Baxter, C. J., Carrari, F., Bauke, A., Overy, S., Hill, S. A., Quick, P. W.*, et al.* (2005) Fruit carbohydrate metabolism in an introgression line of tomato with increased fruit soluble solids. *Plant and Cell Physiology,* **46,** 425-437.

Blumstein, M., Sala, A., Weston, D. J., Holbrook, N. M. and Hopkins, R. (2022) Plant carbohydrate storage: intra- and inter-specific trade-offs reveal a major life history trait. *New Phytologist,* **235,** 2211-2222.

Bryant, N. D., Pu, Y., Tschaplinski, T. J., Tuskan, G. A., Muchero, W., Kalluri, U. C.*, et al.* (2020) Transgenic poplar designed for biofuels. *Trends in Plant Science,* **25,** 881-896.

Charrier, G., Lacointe, A. and Améglio, T. (2018) Dynamic modeling of carbon metabolism during the dormant period accurately predicts the changes in frost hardiness in walnut trees *Juglans regia* L. *Front Plant Sci,* **9,** 1746.

Chen, Z., Gao, K., Su, X., Rao, P. and An, X. (2015) Genome-wide identification of the invertase gene family in *Populus*. *PLoS One,* **10,** e0138540.

Chow, P. S. and Landhäusser, S. M. (2004) A method for routine measurements of total sugar and starch content in woody plant tissues. *Tree Physiology,* **24,** 1129-1136.

Chudy, R. P., Busby, G. M., Binkley, C. S. and Stanton, B. J. (2019) The economics of dedicated hybrid poplar biomass plantations in the western U.S. *Biomass and Bioenergy,* **124,** 114-124.

Dhillon, R. S. and von Wuehlisch, G. (2013) Mitigation of global warming through renewable biomass. *Biomass and Bioenergy,* **48,** 75-89.

Dobbelstein, E., Fink, D., Öner-Sieben, S., Czempik, L. and Lohaus, G. (2018) Seasonal changes of sucrose transporter expression and sugar partitioning in common European tree species. *Tree Physiology,* **39,** 284-299.

Eom, J. S., Cho, J. I., Reinders, A., Lee, S. W., Yoo, Y., Tuan, P. Q.*, et al.* (2011) Impaired function of the tonoplast-localized sucrose transporter in rice, OsSUT2, limits the transport of vacuolar reserve sucrose and affects plant growth. *Plant Physiology,* **157,** 109-119.

Fabisch, T., Gershenzon, J. and Unsicker, S. B. (2019) Specificity of herbivore defense responses in a woody plant, black poplar (*Populus nigra*). *Journal of Chemical Ecology,* **45,** 162-177.

Falk, M. A., Donaldson, J. R., Stevens, M. T., Raffa, K. F. and Lindroth, R. L. (2020) Phenological responses to prior-season defoliation and soil-nutrient availability vary among early- and late-flushing aspen (Populus tremuloides Michx.) genotypes. *Forest Ecology and Management,* **458,** 117771.

Fischer, S., Hanf, S., Frosch, T., Gleixner, G., Popp, J., Trumbore, S.*, et al.* (2015) *Pinus sylvestris* switches respiration substrates under shading but not during drought. *New Phytologist,* **207,** 542-550.

Frost, C. J., Nyamdari, B., Tsai, C.-J. and Harding, S. A. (2012) The tonoplast-localized sucrose transporter in Populus (PtaSUT4) regulates whole-plant water relations, responses to water stress, and photosynthesis. *PLoS One,* **7,** e44467.

Furze, M. E., Huggett, B. A., Aubrecht, D. M., Stolz, C. D., Carbone, M. S. and Richardson, A. D. (2019) Whole-tree nonstructural carbohydrate storage and seasonal dynamics in five temperate species. *New Phytologist,* **221,** 1466-1477.

Gleason, S. M. and Ares, A. (2004) Photosynthesis, carbohydrate storage and survival of a native and an introduced tree species in relation to light and defoliation. *Tree Physiology,* **24,** 1087-1097.

Harding, S. A., Frost, C. J. and Tsai, C.-J. (2020) Defoliation-induced compensatory transpiration is compromised in *SUT4*-RNAi *Populus*. *Plant Direct,* **4,** e00268.

Harding, S. A., Jiang, H. Y., Jeong, M. L., Casado, F. L., Lin, H. W. and Tsai, C. J. (2005) Functional genomics analysis of foliar condensed tannin and phenolic glycoside regulation in natural cottonwood hybrids. *Tree Physiology,* **25,** 1475-1486.

Harding, S. A., Tuma, T. T., Aulakh, K., Ortega, M. A., Ci, D., Ou, Y.*, et al.* (2022) Tonoplast sucrose trafficking modulates starch utilization and water deficit behavior in poplar leaves. *Plant and Cell Physiology,* **63,** 1117-1129.

Hartmann, H. and Trumbore, S. (2016) Understanding the roles of nonstructural carbohydrates in forest trees – from what we can measure to what we want to know. *New Phytologist,* **211,** 386-403.

Herms, D. A. and Mattson, W. J. (1992) The dilemma of plants: To grow or defend. *The Quarterly Review of Biology,* **67,** 283-335.

Hillabrand, R. M., Gordon, H., Hynes, B., Constabel, C. P. and Landhäusser, S. M. (2023) *Populus* root salicinoid phenolic glycosides are not mobilized to support metabolism and regrowth under carbon limited conditions. *Tree Physiol*.

Huang, J., Hammerbacher, A., Gershenzon, J., van Dam, N. M., Sala, A., McDowell, N. G.*, et al.* (2021) Storage of carbon reserves in spruce trees is prioritized over growth in the face of carbon limitation. *Proceedings of the National Academy of Sciences,* **118,** e2023297118.

539 Karp, A. and Shield, I. (2008) Bioenergy from plants and the sustainable yield challenge. *New*
540 *Phytologist,* **179,** 15-32.
541 Kauter, D., Lewandowski, I. and Claupein, W. (2003) Quantity and quality of harvestable
542 biomass from Populus short rotation coppice for solid fuel use—a review of the
543 physiological basis and management influences. *Biomass and Bioenergy,* **24,** 411-427.
544 Klein, T. and Hoch, G. (2015) Tree carbon allocation dynamics determined using a carbon mass
545 balance approach. *New Phytologist,* **205,** 147-159.
546 Kleiner, K. W., Raffa, K. F. and Dickson, R. E. (1999) Partitioning of ^{14}C-labeled photosynthate
547 to allelochemicals and primary metabolites in source and sink leaves of aspen: evidence
548 for secondary metabolite turnover. *Oecologia,* **119,** 408-418.
549 Ko, J.-H., Prassinos, C., Keathley, D., Han, K.-H. and Li, C. (2011) Novel aspects of
550 transcriptional regulation in the winter survival and maintenance mechanism of poplar.
551 *Tree Physiology,* **31,** 208-225.
552 Koch, K. (2004) Sucrose metabolism: regulatory mechanisms and pivotal roles in sugar sensing
553 and plant development. *Current Opinion in Plant Biology,* **7,** 235-246.
554 Kühn, C., Barker, L., Bürkle, L. and Frommer, W.-B. (1999) Update on sucrose transport in
555 higher plants. *Journal of Experimental Botany,* **50,** 935-953.
556 Labrecque, M., Daigle, S. and Olishevska, S. (2023) Comparing biomass yields of various
557 willow cultivars in short-rotation coppice over six growing seasons across a broad
558 climatic gradient in Eastern Canada. *Canadian Journal of Forest Research,* **53,** 533-543.
559 Li, L., Strahwald, J., Hofferbert, H. R., Lübeck, J., Tacke, E., Junghans, H.*, et al.* (2005) DNA
560 variation at the invertase locus invGE/GF is associated with tuber quality traits in
561 populations of potato breeding clones. *Genetics,* **170,** 813-821.
562 Lichtenthaler, H. K. (1987) Chlorophylls and carotenoids: Pigments of photosynthetic
563 biomembranes. In: *Methods Enzymol.* Academic Press, pp. 350-382.
564 Luostarinen, K. and Kauppi, A. (2005) Effects of coppicing on the root and stump carbohydrate
565 dynamics in birches. *New Forests,* **29,** 289-303.
566 Martínez-Vilalta, J., Sala, A., Asensio, D., Galiano, L., Hoch, G., Palacio, S.*, et al.* (2016)
567 Dynamics of non-structural carbohydrates in terrestrial plants: a global synthesis.
568 *Ecological Monographs,* **86,** 495-516.
569 Nieminen, K., Robischon, M., Immanen, J. and Helariutta, Y. (2012) Towards optimizing wood
570 development in bioenergy trees. *New Phytologist,* **194,** 46-53.
571 Noronha, H., Silva, A., Dai, Z., Gallusci, P., Rombolà, A. D., Delrot, S.*, et al.* (2018) A
572 molecular perspective on starch metabolism in woody tissues. *Planta,* **248,** 559-568.
573 Payyavula, R. S., Tay, K. H. C., Tsai, C.-J. and Harding, S. A. (2011) The sucrose transporter
574 family in Populus: The importance of a tonoplast PtaSUT4 to biomass and carbon
575 partitioning. *Plant Journal,* **65,** 757-770.
576 Peng, D., Xue, L.-J., Gu, X., Leebens-Mack, J. H. and Tsai, C.-J. (2014) Bayesian phylogeny of
577 sucrose transporters: Ancient origins, differential expansion and convergent evolution in
578 monocots and dicots. *Frontiers in Plant Science,* **5,** 615.
579 Piper, F. I. and Fajardo, A. (2016) Carbon dynamics of *Acer pseudoplatanus* seedlings under
580 drought and complete darkness. *Tree Physiology,* **36,** 1400-1408.
581 Porter, L. J., Hrstich, L. N. and Chan, B. G. (1986) The conversion of procyanidins and
582 prodelphinidins to cyanidin and delphinidin. *Phytochemistry,* **25,** 223-230.

583 Proe, M. F., Craig, J., Griffiths, J., Wilson, A. and Reid, E. (1999) Comparison of biomass
584 production in coppice and single stem woodland management systems on an imperfectly
585 drained gley soil in central Scotland. *Biomass and Bioenergy,* **17,** 141-151.
586 Ragauskas, A. J., Williams, C. K., Davison, B. H., Britovsek, G., Cairney, J., Eckert, C. A*., et al.*
587 (2006) The path forward for biofuels and biomaterials. *Science,* **311,** 484-489.
588 Regier, N., Streb, S., Zeeman, S. C. and Frey, B. (2010) Seasonal changes in starch and sugar
589 content of poplar (Populus deltoides × nigra cv. Dorskamp) and the impact of stem
590 girdling on carbohydrate allocation to roots. *Tree Physiology,* **30,** 979-987.
591 Roitsch, T. and González, M.-C. (2004) Function and regulation of plant invertases: sweet
592 sensations. *Trends in Plant Science,* **9,** 606-613.
593 Ruan, Y.-L. (2014) Sucrose metabolism: Gateway to diverse carbon use and sugar signaling.
594 *Annual Review of Plant Biology,* **65,** 33-67.
595 Sala, A., Woodruff, D. R. and Meinzer, F. C. (2012) Carbon dynamics in trees: feast or famine?
596 *Tree Physiology,* **32,** 764-775.
597 Schädel, C., Blöchl, A., Richter, A. and Hoch, G. (2009) Short-term dynamics of nonstructural
598 carbohydrates and hemicelluloses in young branches of temperate forest trees during bud
599 break. *Tree Physiology,* **29,** 901-911.
600 Schneider, S., Hulpke, S., Schulz, A., Yaron, I., Holl, J., Imlau, A*., et al.* (2012) Vacuoles release
601 sucrose via tonoplast-localised SUC4-type transporters. *Plant Biology,* **14,** 325-336.
602 Schulz, A., Beyhl, D., Marten, I., Wormit, A., Neuhaus, E., Poschet, G*., et al.* (2011) Proton-
603 driven sucrose symport and antiport are provided by the vacuolar transporters SUC4 and
604 TMT1/2. *Plant Journal,* **68,** 129-136.
605 Sekhon, R. S., Breitzman, M. W., Silva, R. R., Santoro, N., Rooney, W. L., de Leon, N*., et al.*
606 (2016) Stover composition in maize and sorghum reveals remarkable genetic variation
607 and plasticity for carbohydrate accumulation. *Frontiers in Plant Science,* **7**.
608 Sevanto, S., Mcdowell, N. G., Dickman, L. T., Pangle, R. and Pockman, W. T. (2014) How do
609 trees die? A test of the hydraulic failure and carbon starvation hypotheses. *Plant, Cell &*
610 *Environment,* **37,** 153-161.
611 Siebrecht, S. and Tischner, R. (1999) Changes in the xylem exudate composition of poplar
612 (Populus tremula x P. alba)—dependent on the nitrogen and potassium supply. *Journal of*
613 *Experimental Botany,* **50,** 1797-1806.
614 Smith, A. M. and Stitt, M. (2007) Coordination of carbon supply and plant growth. *Plant Cell*
615 *and Environment,* **30,** 1126-1149.
616 Tarkowski, Ł., P. and Van den Ende, W. (2015) Cold tolerance triggered by soluble sugars: a
617 multifaceted countermeasure. *Front Plant Sci,* **6,** 203.
618 Tixier, A., Orozco, J., Roxas, A. A., Earles, J. M. and Zwieniecki, M. A. (2018) Diurnal
619 variation in nonstructural carbohydrate storage in trees: Remobilization and vertical
620 mixing. *Plant Physiology,* **178,** 1602-1613.
621 Tsai, C.-J., Harding, S. A., Tschaplinski, T. J., Lindroth, R. L. and Yuan, Y. (2006) Genome-
622 wide analysis of the structural genes regulating defense phenylpropanoid metabolism in
623 Populus. *New Phytologist,* **172,** 47-62.
624 Tschaplinski, T. J. and Blake, T. J. (1989) Photosynthetic reinvigoration of leaves following
625 shoot decapitation and accelerated growth of coppice shoots. *Physiologia Plantarum,* **75,**
626 157-165.
627 Wang, W., Talide, L., Viljamaa, S. and Niittylä, T. (2022) Aspen growth is not limited by starch
628 reserves. *Current Biology,* **32,** 3619-3627.e3614.

629 Wiley, E., King, C. M. and Landhäusser, S. M. (2019) Identifying the relevant carbohydrate
630 storage pools available for remobilization in aspen roots. *Tree Physiology,* **39,** 1109-
631 1120.
632 Wormit, A., Trentmann, O., Feifer, I., Lohr, C., Tjaden, J., Meyer, S.*, et al.* (2006) Molecular
633 identification and physiological characterization of a novel monosaccharide transporter
634 from Arabidopsis involved in vacuolar sugar transport. *Plant Cell,* **18,** 3476-3490.
635 Xu, Q., Chen, S., Yunjuan, R., Chen, S. and Liesche, J. (2017) Regulation of Sucrose
636 Transporters and Phloem Loading in Response to Environmental Cues. *Plant Physiology,*
637 **176,** 930-945.
638 Xue, L.-J., Frost, C. J., Tsai, C.-J. and Harding, S. A. (2016) Drought response transcriptomics
639 are altered in poplar with reduced tonoplast sucrose transporter expression. *Scientific*
640 *Reports,* **6,** 33655.
641 Zhang, C., Han, L., Slewinski, T. L., Sun, J., Zhang, J., Wang, Z.-Y.*, et al.* (2014) Symplastic
642 phloem loading in poplar. *Plant Physiology,* **166,** 306-313.
643 Zhang, J., Yang, Y., Zheng, K., Xie, M., Feng, K., Jawdy, S. S.*, et al.* (2018) Genome-wide
644 association studies and expression-based quantitative trait loci analyses reveal roles of
645 HCT2 in caffeoylquinic acid biosynthesis and its regulation by defense-responsive
646 transcription factors in Populus. *New Phytologist,* **220,** 502-516.
647 Zhou, X., Jacobs, T. B., Xue, L.-J., Harding, S. A. and Tsai, C.-J. (2015) Exploiting SNPs for
648 biallelic CRISPR mutations in the outcrossing woody perennial *Populus* reveals 4-
649 coumarate:CoA ligase specificity and redundancy. *New Phytologist,* **208,** 298-301.
650
651

652 **Figure Legends**

653 **FIGURE 1:** Epicormic bud emergence and growth following coppicing.

654 (A-B) Representative images of *sut4* and control poplar stools under summer (A) and winter (B)

655 conditions immediately after coppicing (t= 0), during epicormic bud expansion (t=1), and during

656 sprout growth (t=2). (C-D) Bud emergence after summer (C) and winter (D) coppicing. Black

657 and grey represent control and *sut4* plants, respectively. Values are means ± SD of n = 8

658 biological replicates. The effects of time (t), genotype (g), or their interaction (t × g) were

659 assessed by a repeated measures two-way ANOVA. (E) Length of largest (dominant) epicormic

660 bud at t=1. Data are mean ± SD of n = 8 - 12 biological replicates. Statistical significance was

661 determined by Student's t test between control and *sut4* plants. (F) Sprout biomass at t=2. Data

662 are mean ± SD of n = 8 - 12 biological replicates. Statistical significance was determined by

663 Student's *t* test between control and *sut4* plants. ns, nonsignificant; *, $P \leq 0.05$; **, $P \leq 0.01$;

664 ***, $P \leq 0.001$.

665

666 **FIGURE 2:** Non-structural carbohydrate abundance dynamics following coppicing.

667 (A) Sucrose, (B) Hexose (sum of fructose and glucose), and (C) Starch. Black and grey are for

668 control and *sut4* plants, respectively. Values are mean ± SD of $n = 10$ biological replicates. The

669 effects of time (t), genotype (g) or their interaction (t × g) were assessed by repeated measures

670 two-way ANOVA. Statistical significance for root starch levels at t=2 was determined by

671 Student's *t* test between control and *sut4* plants. ns, nonsignificant; *, $P \leq 0.05$; **, $P \leq 0.01$;

672 ***, $P \leq 0.001$.

673

674 **FIGURE 3:** Epicormic bud length as a function of bark carbohydrate depletion under summer

675 and winter conditions.

676 (A-B) Bud length at t=1 versus sucrose (A) or starch (B) depletion between t=0 and t=1. Linear

677 regression trendlines are depicted in blue and red for control and *sut4*, respectively. Shading

678 highlights the 95% confidence intervals.

679

680 **FIGURE 4:** Xylem sap metabolites.

681 (A) Sucrose, (B) Hexoses, (C-D) Abundance ranking of the most prevalent metabolites after

682 sucrose and hexose in control and *sut4* sap in summer (C) and winter (D). Krebs cycle

683 intermediates are in green and amino acids are in brown colors, with control and *sut4* in darker

684 and lighter shading, respectively. Values represent the mean ± SE (n = 8-10). Statistical

685 significance between genotypes was determined by Student's *t* test. *, $P \leq 0.05$; **, $P \leq 0.01$;

686 ***, $P \leq 0.001$.

687

688 **FIGURE 5:** Post coppice metabolic reprogramming in bark and xylem.

689 Heatmap depiction of $\log_2$-transformed metabolite response ratio (*sut4*/control) in bark (A) and

690 xylem (B). Blue and red colors indicate decreased or increased metabolite abundance in mutants,

691 while grey indicates not detected. Significance between genotypes was obtained by Student's *t*-

692 test and is indicated in bold underlined ($P \leq 0.01$) or bold font ($P \leq 0.05$).

693

694 **FIGURE 6:** Bark secondary metabolites

695 (A) Chlorogenic acids (sum of caffeoyl-quinate isomers), (B) salicortin, (C) tremulacin, and (D)

696 condensed tannins. Values represent the mean ± SD of $n = 8$ biological replicates. The effects of

697 time (t), genotype (g) or their interaction were assessed by repeated measures two-way ANOVA.

698 *, $P \leq 0.05$; **, $P \leq 0.01$; ***, $P \leq 0.001$.

699

700 **FIGURE 7:** Bark chlorophyll content.

701 Changes in bark chlorophyll following summer (A) and winter (B) coppicing. Black and grey are

702 for control and *sut4* plants, respectively. Data are presented as the mean ± SD ($n = 10$). The

703 effects of time (t), genotype (g) or their interaction were assessed by repeated measures two-way

704 ANOVA. *, $P \leq 0.05$; ***, $P \leq 0.001$.

Table 1. Total biomass of new sprout growth following coppicing in control and *sut4* poplar.

	Summer		Winter	
	Control	*sut4*	Control	*sut4*
Tissue dry mass (g)				
Leaf	10.97 ± 2.80	16.15 ± 3.40**	10.35 ± 1.55	9.55 ± 1.74
Stem	5.37 ± 1.35	7.55 ± 1.76**	5.22 ± 0.96	4.89 ± 0.78
Root[1]	11.47 ± 2.37	11.55 ± 2.76	10.88 ± 1.17	9.42 ± 1.42

Values represent mean and SD of $n = 6 – 11$ biological replicates. Student's *t*-test was used to determine statistical significance between genotypes. **, $P \leq 0.01$; ***, $P \leq 0.001$.
[1]Root biomass represent total growth pre- and post-coppicing.

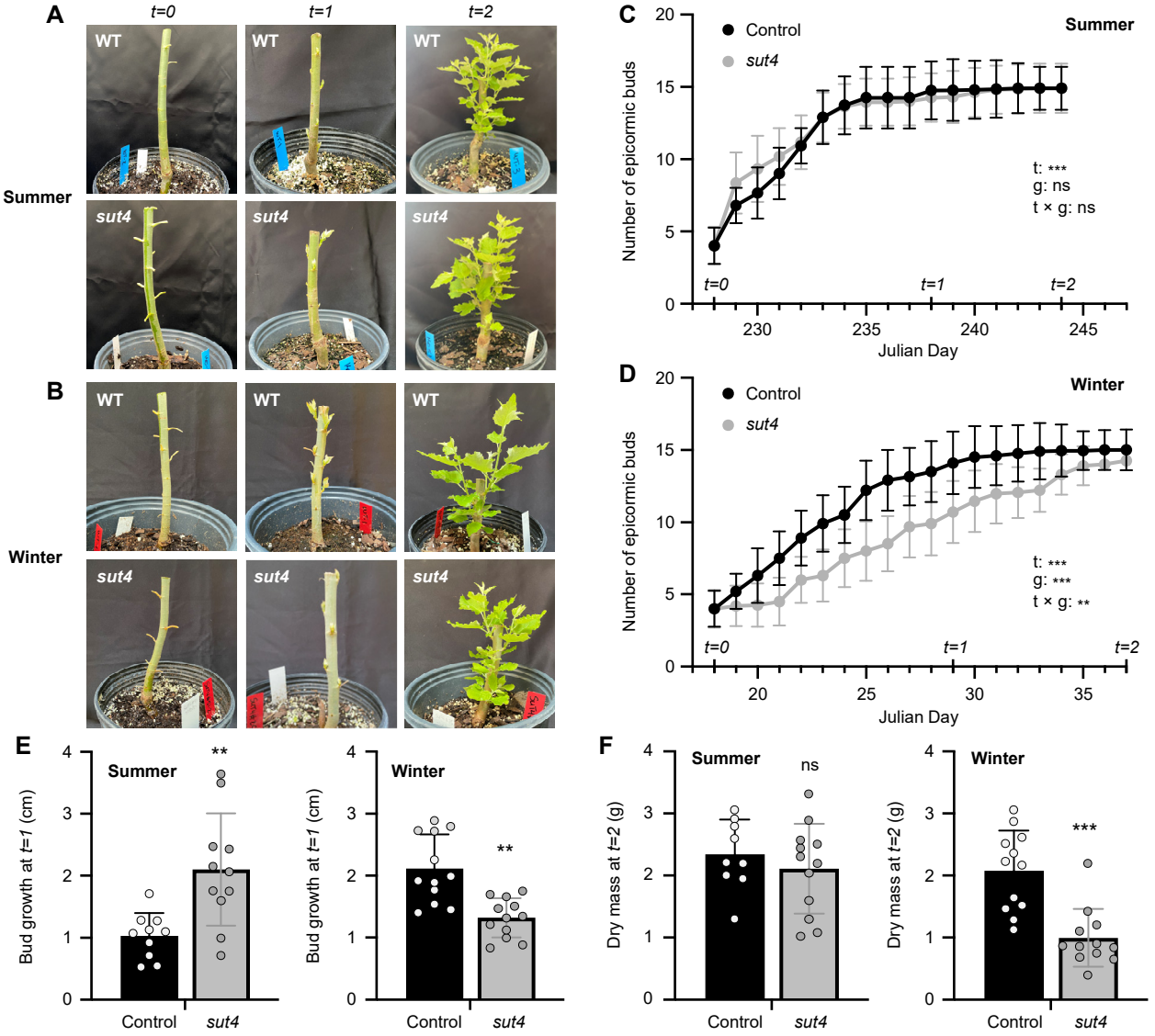

FIGURE 1. Epicormic bud emergence and growth following coppicing.
(A-B) Representative images of *sut4* and control poplar stools under summer (A) and winter (B) conditions immediately after coppicing (t=0), during epicormic bud expansion (t=1), and during sprout growth (t=2). (C-D) Bud emergence after summer (C) and winter (D) coppicing. Black and grey represent control and *sut4* plants, respectively. Values are means ± SD of n = 8 biological replicates. The effects of genotype or time were assessed by a repeated measures two-way ANOVA and indicated by *P* values. t, time; g, genotype; t × g, time × genotype interaction. (E) Length of largest (dominant) epicormic bud at t=1. Data are mean ± SD of n = 8-12 biological replicates. Statistical significance was determined by Student's *t* test between control and *sut4* plants. (F) Sprout biomass at t=2. Data are mean ± SD of n = 8-12 biological replicates. Statistical significance was determined by Student's *t* test between control and *sut4* plants. ns, nonsignificant; *, $P \leq 0.05$; **, $P \leq 0.01$; ***, $P \leq 0.001$.

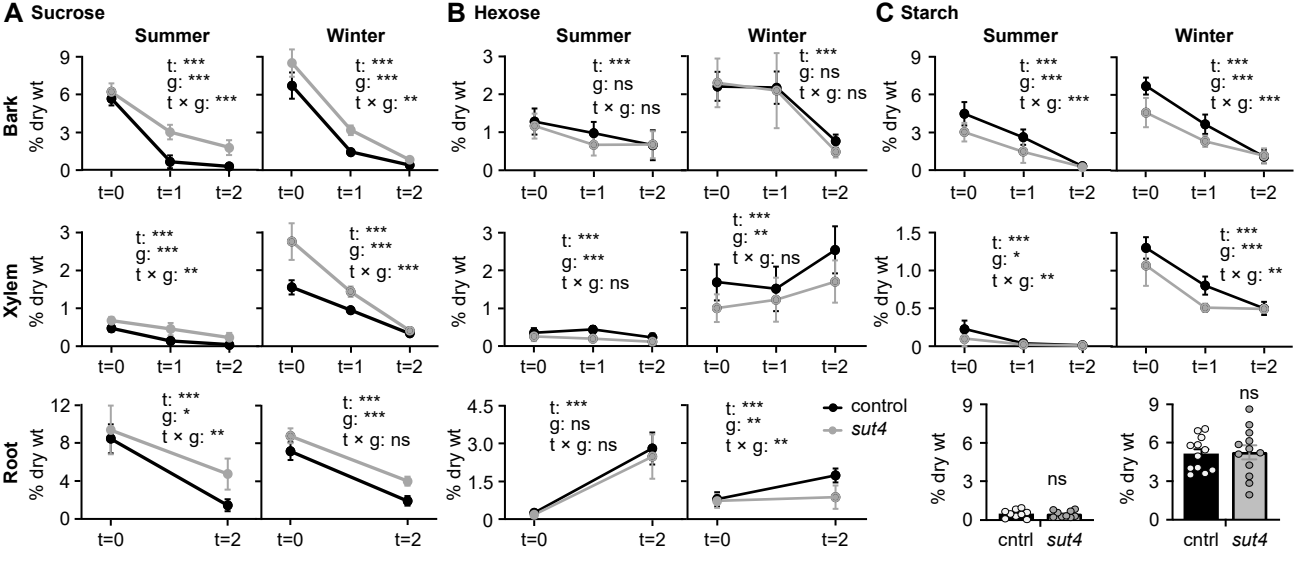

FIGURE 2: Non-structural carbohydrate abundance dynamics following coppicing.
(A) Sucrose, (B) Hexose (sum of fructose and glucose), and (C) Starch. Black and grey are for control and *sut4* plants, respectively. Values are mean ± SD of $n = 10$ biological replicates. The effects of time (t), genotype (g) or their interaction (t × g) were assessed by repeated measures two-way ANOVA. Statistical significance for root starch levels at t=2 was determined by Student's *t* test between control and *sut4* plants. ns, nonsignificant; *, $P \leq 0.05$; **, $P \leq 0.01$; ***, $P \leq 0.001$.

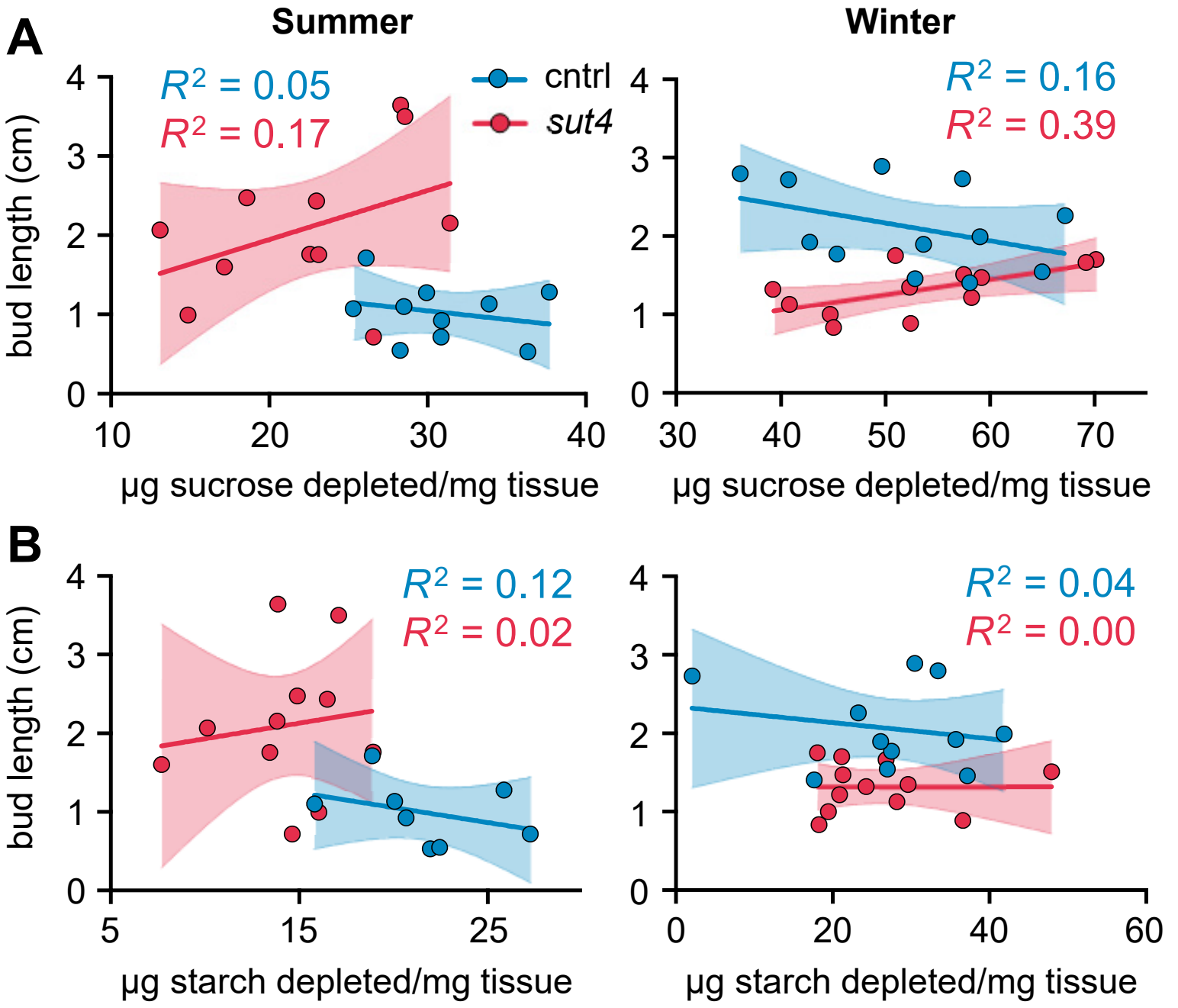

FIGURE 3: Epicormic bud length as a function of bark carbohydrate depletion under summer and winter conditions.
(A-B) Bud length at t=1 versus sucrose (A) or starch (B) depletion between t=0 and t=1. Linear regression trendlines are depicted in blue and red for control and *sut4*, respectively. Shading highlights the 95% confidence intervals.

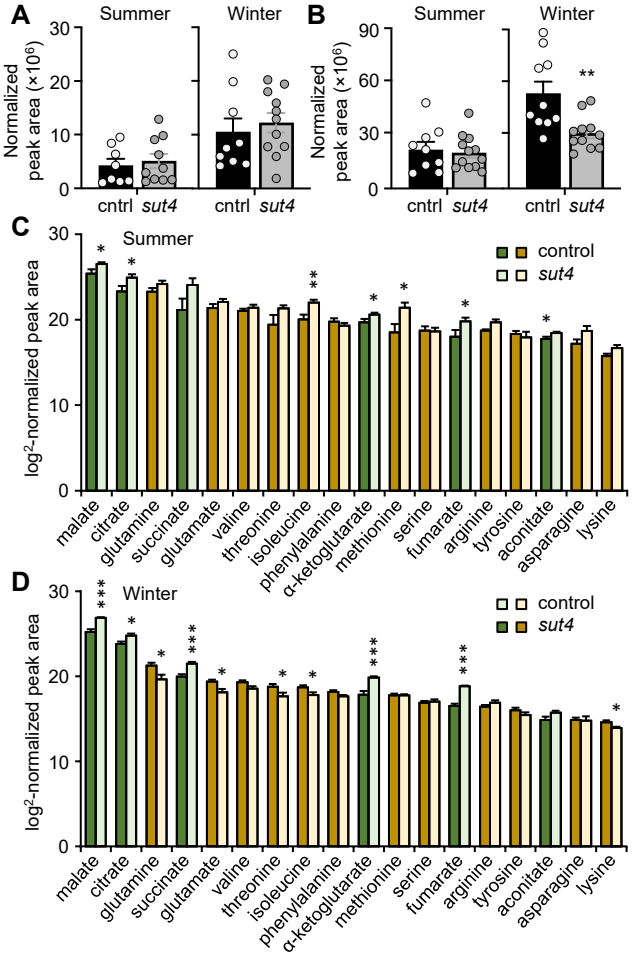

FIGURE 4: Xylem sap metabolites.
(A) Sucrose, (B) hexoses, (C-D) abundance ranking of the most prevalent metabolites after sucrose and hexose in control and *sut4* sap in summer (C) and winter (D). Krebs cycle intermediates are in green and amino acids are in brown colors, with control and *sut4* in darker and lighter shading, respectively. Values represent the mean ± SE (n = 8-10). Statistical significance between genotypes was determined by Student's t test. *, $P \leq 0.05$; **, $P \leq 0.01$; ***, $P \leq 0.001$.

-2 -1 0 1 2

		Bark						Xylem					
		Summer			Winter			Summer			Winter		
		t=0	t=1	t=2	t=0	t=1	t=2	t=0	t=1	t=2	t=0	t=1	t=2
amino acids	glutamate	-0.01	0.03	**0.35**	**-0.74**	**0.73**	**0.84**	-0.19	-0.54		-0.35	0.19	0.09
	threonine		-0.01	**0.58**	-0.16	-0.05	**0.78**				0.14	0.11	-0.03
	valine		0.17	**0.67**	-0.41	0.28	**0.66**				-0.22	-0.06	-0.12
	aspartate	**0.76**	**0.53**	**0.72**	-0.07	**0.53**	**0.66**				-0.01	0.12	-0.12
	lysine		0.17	**0.53**	-0.17	0.26	**0.52**						
	γ-aminobutyrate	**0.78**	**0.36**	**0.61**	**0.46**	**0.49**	**0.37**		0.07	-0.03	0.51	**0.69**	-0.08
	glutamine	0.28	-0.08	0.70	-0.05	**0.34**	0.21		-0.48	0.29	-0.41	-0.20	-0.16
	serine		0.30	**0.73**	-0.21	-0.04	0.10				-0.06	0.38	-0.61
	asparagine		1.13	**1.11**		0.79	-0.36		0.35	0.73		0.28	-0.03
	phenylalanine							0.24			**-0.57**	**0.74**	**0.36**
	arginine											**1.41**	0.22
Krebs cycle	citric acid	0.34	-0.02	0.12	**0.50**	**0.58**	**1.55**	0.05	0.09	0.34	**0.78**	**1.37**	**1.60**
	malic acid	-0.10	0.00	0.02	0.07	**0.53**	**0.50**	0.18	-0.07	-0.30	**0.62**	**0.82**	**0.83**
	succinic acid	0.00	**0.25**	0.11	-0.39	-0.16	0.17	-1.04	-0.68	-0.41	-0.11	-0.08	**-0.43**
phenolics	catechin	**-0.74**	**-0.61**	**-0.40**	**-0.56**	**-0.19**	0.03		-0.11	0.23	-0.70	**-1.42**	**-0.81**
	cinnamic acid	0.13	**0.27**	**0.24**	0.26	**0.43**	-0.03						
	shikimic acid	**0.43**	**-0.61**	**-0.71**	0.16	**-0.42**	**-0.55**				**-0.53**	-0.18	**-0.66**
	quinic acid	**-0.90**	-1.02	**-0.74**	**-0.76**	**-0.73**	**-0.69**	**-1.13**	**-0.83**	**-1.40**	**-0.52**	**-0.42**	**-1.13**
	p-coumaric acid				-0.17	**-0.60**	**-1.37**						
sugars and derivatives	sucrose	**0.11**	**0.80**	**1.15**	**0.34**	**1.12**	**1.27**	**0.51**	**2.47**	**2.40**	**0.80**	**1.68**	**0.69**
	melezitose	-0.05	0.08	0.05	**-0.74**	**0.56**	**0.57**						
	galactinol	0.29			**0.47**	0.11	**0.47**						
	arabinofuranose	0.07	0.35	0.28	**0.24**	0.18	**0.31**						
	fructose	0.03	-0.12	0.40	0.23	**0.28**	-0.16	-0.25	**-0.78**	-0.46	**-0.53**	0.07	**-0.59**
	myo-inositol	**0.33**	-0.13	-0.22	**0.27**	-0.13	-0.41	0.25	0.61	-0.01	**0.34**	**0.43**	0.13
	lactose	-0.32	-0.42	**-0.71**	**-0.38**	**-0.34**	**-0.65**						
	trehalose	**-1.08**	**-0.94**	**-0.88**	0.16	0.05	**-0.75**	-0.40			**-0.52**	-0.41	**-0.57**
	glucose	-0.20	**-1.09**	-0.48	-0.09	**-0.72**	**-1.13**	**-0.58**	**-1.23**	**-1.08**	**-0.76**	**-0.72**	**-0.89**
	raffinose	**1.06**	**-0.75**	**-1.23**	**2.07**	-0.51	**-1.15**						-0.07
	sorbose	0.08	-0.15	0.19	-0.13	0.56							
other	mucic acid	0.05	-0.07		**1.17**	**1.70**	**1.05**				**1.63**		**0.83**
	gluconic acid	-0.21			**1.24**	**1.16**	**0.43**				**1.90**	**1.81**	1.06

FIGURE 5: Post coppice metabolic reprogramming in bark and xylem. Heatmap depiction of $\log_2$-transformed metabolite response ratio (*sut4*/control) in bark (A) and xylem (B). Blue and red colors indicate decreased or increased metabolite abundance in mutants, while grey indicates not detected. Significance between genotypes was obtained by Student's *t*-test and is indicated in bold underlined ($P \leq 0.01$) or bold font ($P \leq 0.05$).

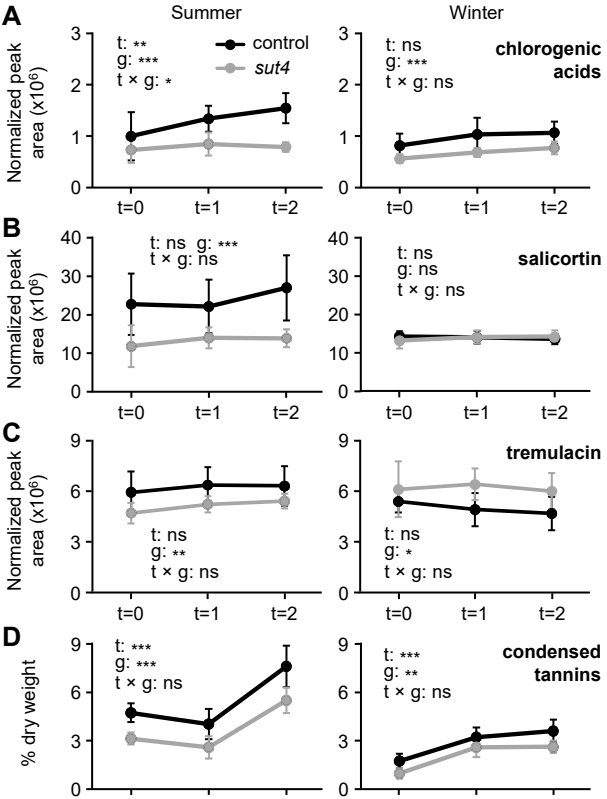

FIGURE 6: Bark secondary metabolites
(A) Chlorogenic acids (sum of caffeoyl-quinate isomers), (B) salicortin, (C) tremulacin, and (D), condensed tannins. Values represent the mean ± SD of $n = 8$ biological replicates. The effects of time (t), genotype (g) or their interaction were assessed by repeated measures two-way ANOVA. *, $P \leq 0.05$; **, $P \leq 0.01$; ***, $P \leq 0.001$.

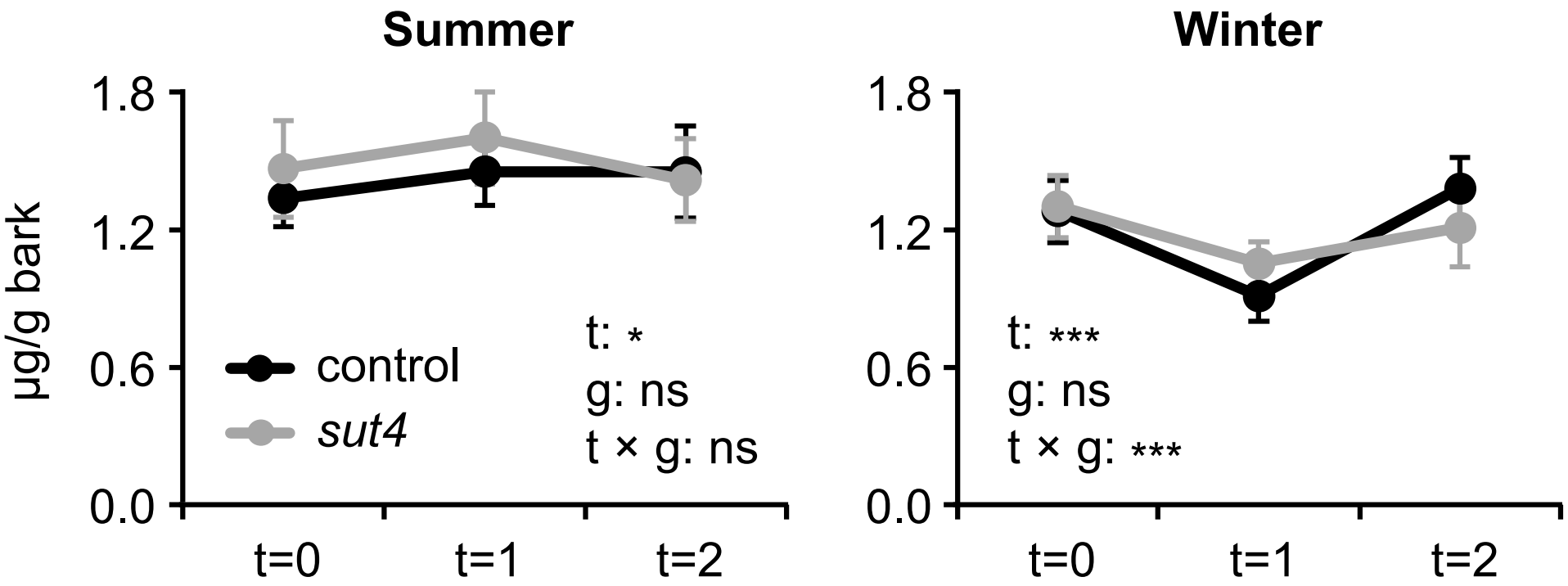

FIGURE 7: Bark chlorophyll content.
Changes in bark chlorophyll following summer (A) and winter (B) coppicing. Black and grey are for control and *sut4* plants, respectively. Data are presented as the mean ± SD (n = 10). The effects of time (t), genotype (g) or their interaction were assessed by repeated measures two-way ANOVA. *, $P \leq 0.05$; ***, $P \leq 0.001$.